

Proceedings Paper

Asymmetric transfer hydrogenation of aryl heteroaryl ketones and *o*-hydroxyphenyl ketones using Noyori-Ikariya catalysts [†]

Ye Zheng;^a Jaime A. Martinez-Acosta;^b Mohammed Khimji;^a Luiz C. A. Barbosa;^b Guy J. Clarkson;^a and Martin Wills.^{a*}

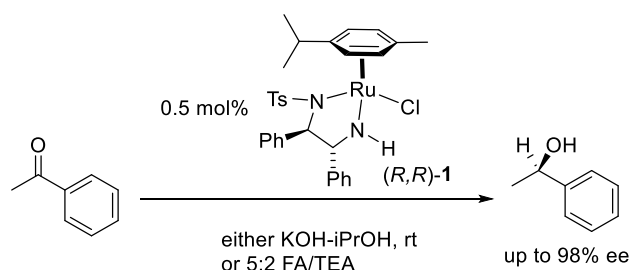
¹ ^a Department of Chemistry, The University of Warwick, Coventry, CV4 7AL, UK

^b Universidade Federal de Minas Gerais, Dept Chem, ICEX, Av Presidente Antonio Carlos 6627, Campus Pampulha, BR-31270901 Belo Horizonte, MG, Brazil.

[†] Presented at the 25th International Electronic Conference on Synthetic Organic Chemistry, 15-30 November 2021; Available online: <https://ecsoc-25.sciforum.net/>.

Abstract: A single paragraph of about 100 words to give a brief introduction to your work.

In 1995, Noyori and co-workers made a breakthrough with their design of practical ruthenium-based catalysts, which combined the homochiral TsDPEN ligand with a Ru(II) arene.¹ Using (*R,R*)-1 at a loading of 0.5 mol% in either KOH-*i*PrOH or the azeotropic mixture of formic acid-triethylamine (FA:TEA, 5:2 molar ratio), the reduction of acetophenone was achieved in up to 98% ee (Figure 1).



Citation: Lastname, F.; Lastname, F.; Lastname, F. Title. *Chem. Proc.* 2021, 3, x. <https://doi.org/10.3390/xxxxx>

Published: date

Publisher's Note: MDPI stays neutral with regard to jurisdictional claims in published maps and institutional affiliations.



Copyright: © 2021 by the authors. Submitted for possible open access publication under the terms and conditions of the Creative Commons Attribution (CC BY) license (<http://creativecommons.org/licenses/by/4.0/>).

Figure 1. Asymmetric Transfer Hydrogenation (ATH) with Noyori-Ikariya catalysts.

The mechanism for the asymmetric transfer hydrogenation (ATH) with Noyori-Ikariya catalysts is now well-established (Figure 2).² The precatalyst can be activated by elimination of HCl to form a 16-electron neutral Ru(II) complex. Then the 16-electron complex abstracts two hydrogen atoms from the hydrogen donor, such as isopropanol, a formic acid/triethylamine (FA/TEA) mixture or sodium formate, to form a hydride that contains an 18-electron Ru(II) centre. Finally, the two hydrogen atoms are transferred to the C=O group and reduce ketone substrates into chiral alcohol products. Meanwhile, the 16-electron neutral Ru(II) complex is regenerated and can restart the catalytic cycle. The six-membered transition state can be stabilized by the combination of electrostatic interactions and steric effects. Edge/face (or CH/ π) electrostatic interaction makes electron-rich aryl group of a substrate favour the position adjacent to the η^6 -arene ring of the catalyst

(Figure 3), while the large group and electron group favours the position distal to η^6 -arene ring (Figure 4).

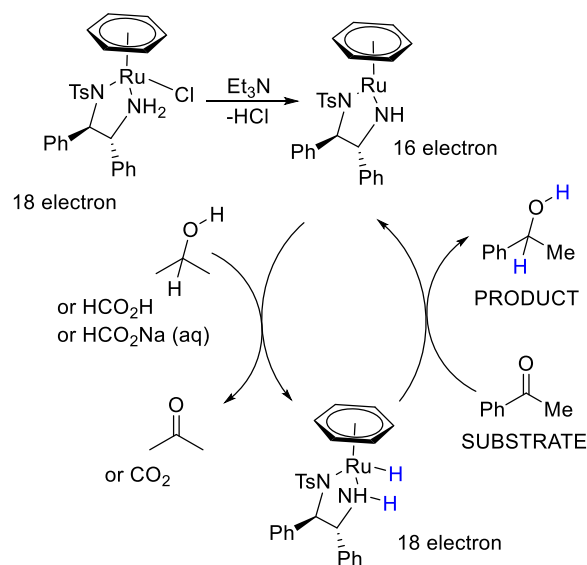


Figure 2. Mechanism of hydrogen transfer with Noyori-Ikariya catalysts.

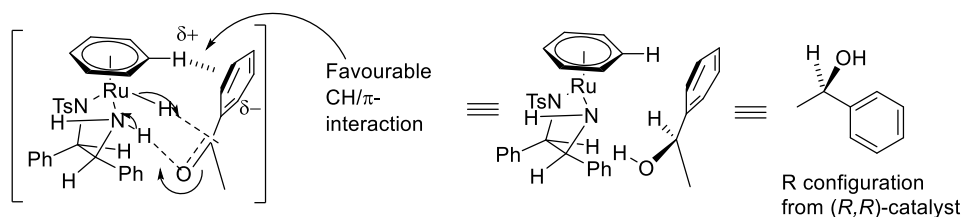


Figure 3. Interaction of substrate with η^6 -arene ring.

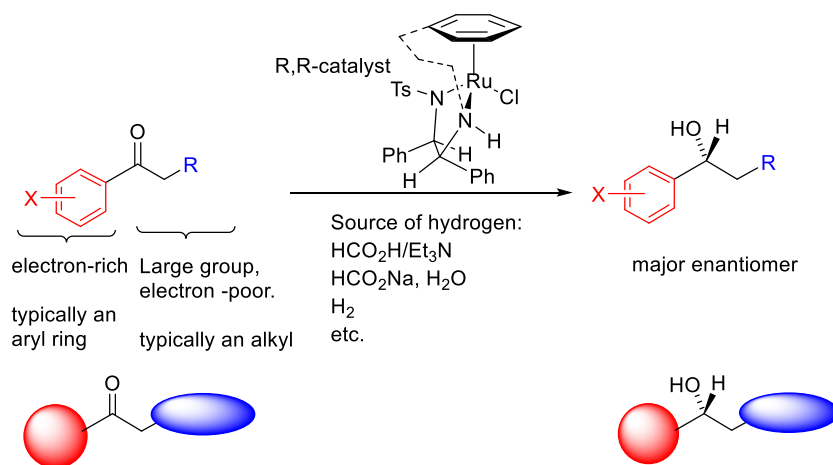


Figure 4. Summary of stereocontrol features in ATH using Noyori-Ikariya catalysts.

Noyori [(arene)Ru(TsDPEN)Cl] catalysts with different arene rings are shown below (Figure 5).³ The reactivity of Noyori type catalysts in ATH reactions is changed when the arene ligand is different, activity following the order benzene > *p*-cymene \approx mesitylene > hexamethylbenzene.

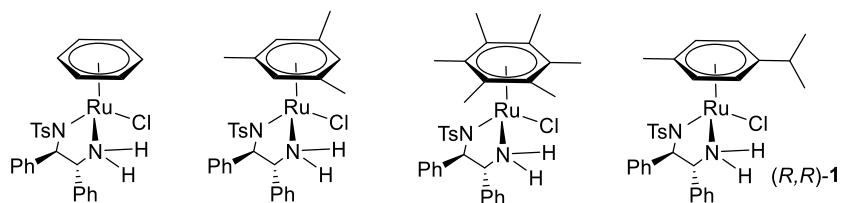


Figure 5. Variation of the η^6 -arene ring in Noyori-Ikariya catalysts.

A new class of “tethered” ruthenium (II) catalyst was introduced by Wills *et al.* (Figure 6).⁴ In some cases these exhibit improved activity over the non-tethered versions, which allows a reduction of catalyst loading and reaction times.

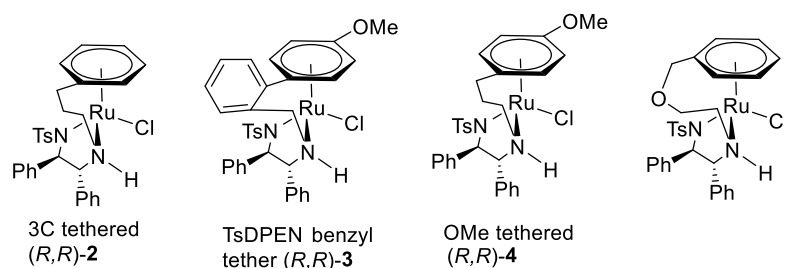


Figure 6. Tethered catalysts introduced by Wills *et al.*

ATH of some benzophenone derivatives⁵ and heterocyclic ketones⁶ has been reported. The electronic differences between two phenyl rings caused by the electron-donating *p*-OMe group and electron-withdrawing *p*-CN group make *p*-OMe substituted phenyl ring adopt the position proximal to the η^6 -arene. Out-of-plane aromatic rings with one or two *ortho*-substituent groups favour positioning distal to η^6 -arene and results in forming alcohol products with very high ees (Figure 7).

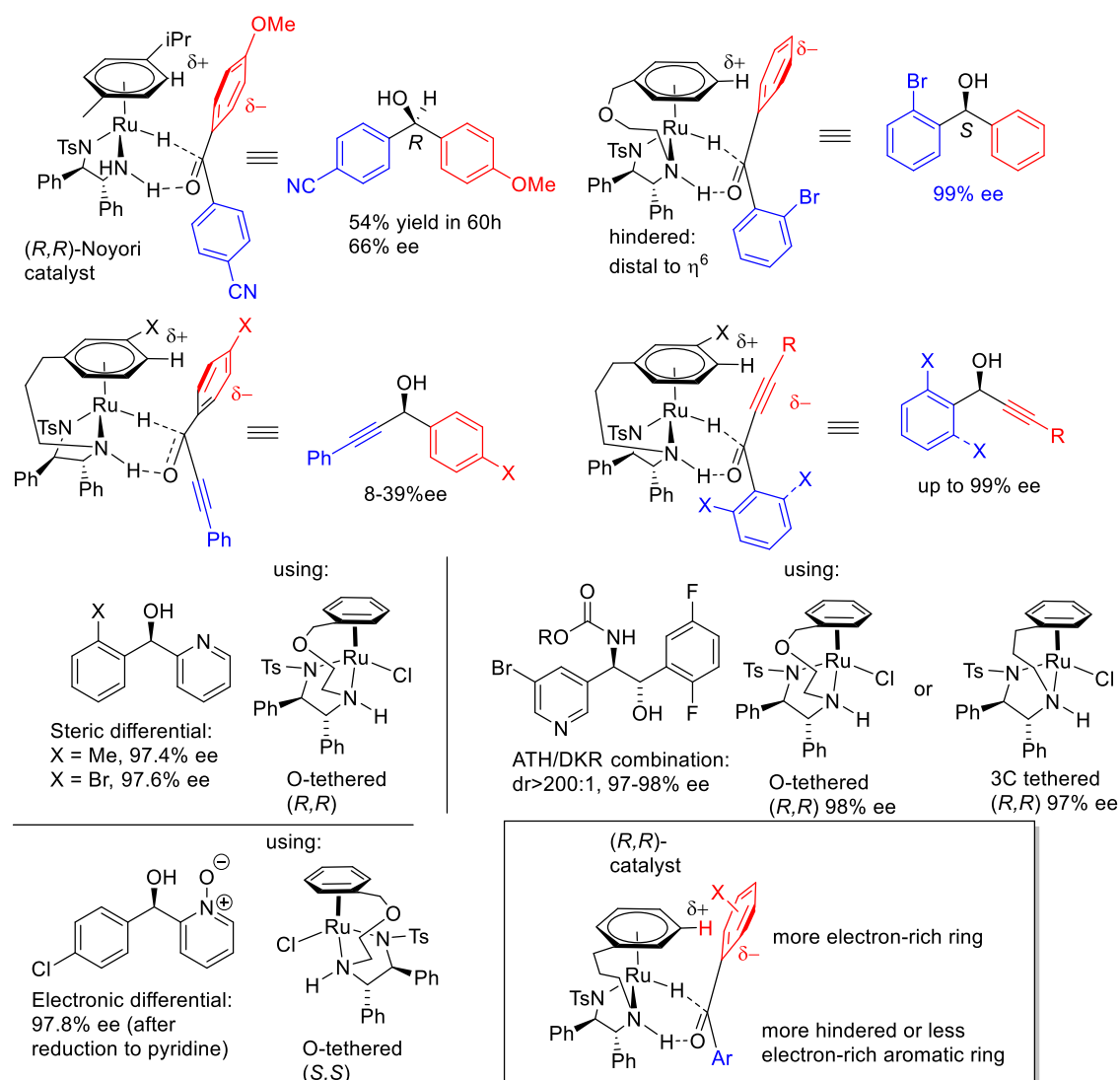


Figure 7. Examples of ATH of benzophenone derivatives and heterocyclic ketones using Noyori-Ikariya catalysts.

We have studied ATH of *ortho*-hydroxyphenyl acetophenone derivatives with 4 different tethered catalysts (Figure 8).⁷ *(R,R)*-3C-tethered catalyst 2 was found to be the most active of the series tested initially with *ortho*-hydroxybenzophenone.

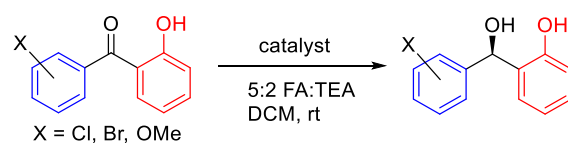


Figure 8. ATH of *ortho*-hydroxy benzophenones using tethered ATH complexes.

The configuration of alcohol product 5 was confirmed after methylation by comparison of the HPLC of reduction product 6, the configuration of which is known in the literature (Figure 9).

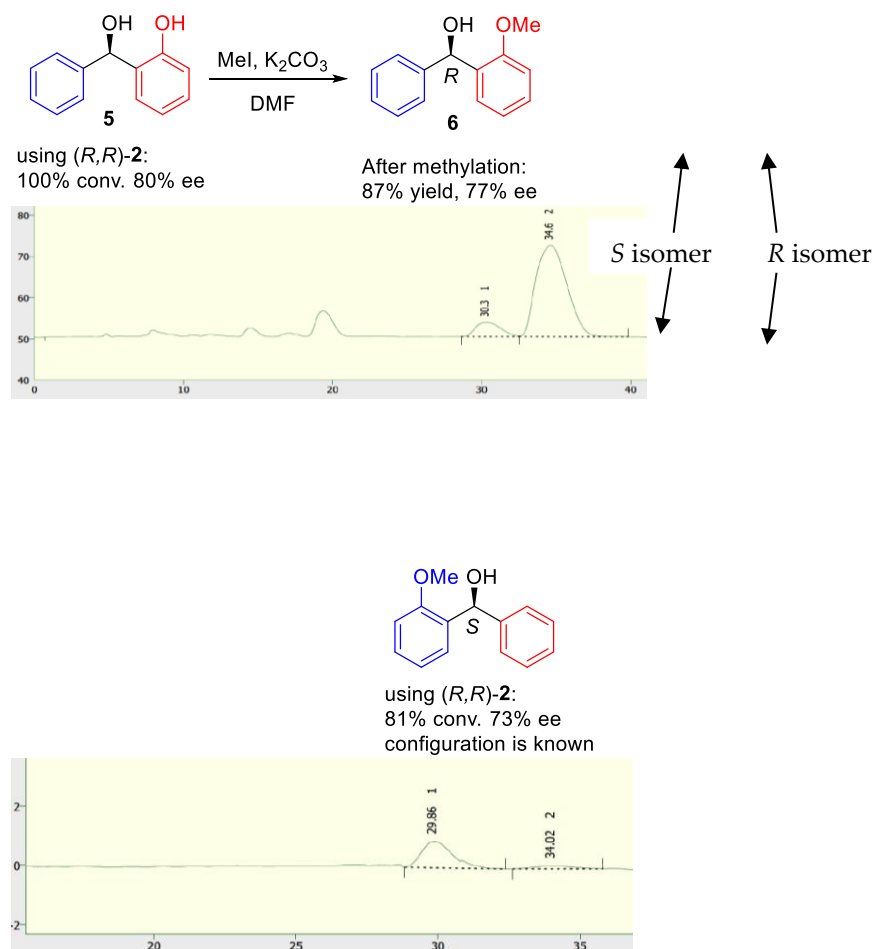


Figure 9. Determination of product configuration in ATH of *ortho*-hydroxy benzophenones.

We also completed the ATH of a range of *ortho*-hydroxyphenyl acetophenone derivatives using four catalysts and found that most of them can provide products in good yield and high ee (Figure 10). The electron-rich *ortho*-hydroxyphenyl group can generate an electrostatic interaction with η^6 -arene ring in the complex, whereas the hindered opposing aromatic ring can be in a position that is far from the η^6 -arene ring (Figure 11). Therefore, the combination of *ortho*-OH directing group and steric effect provide products with high ees. The application could also be extended to a series of amide-containing benzophenones (Figure 12).

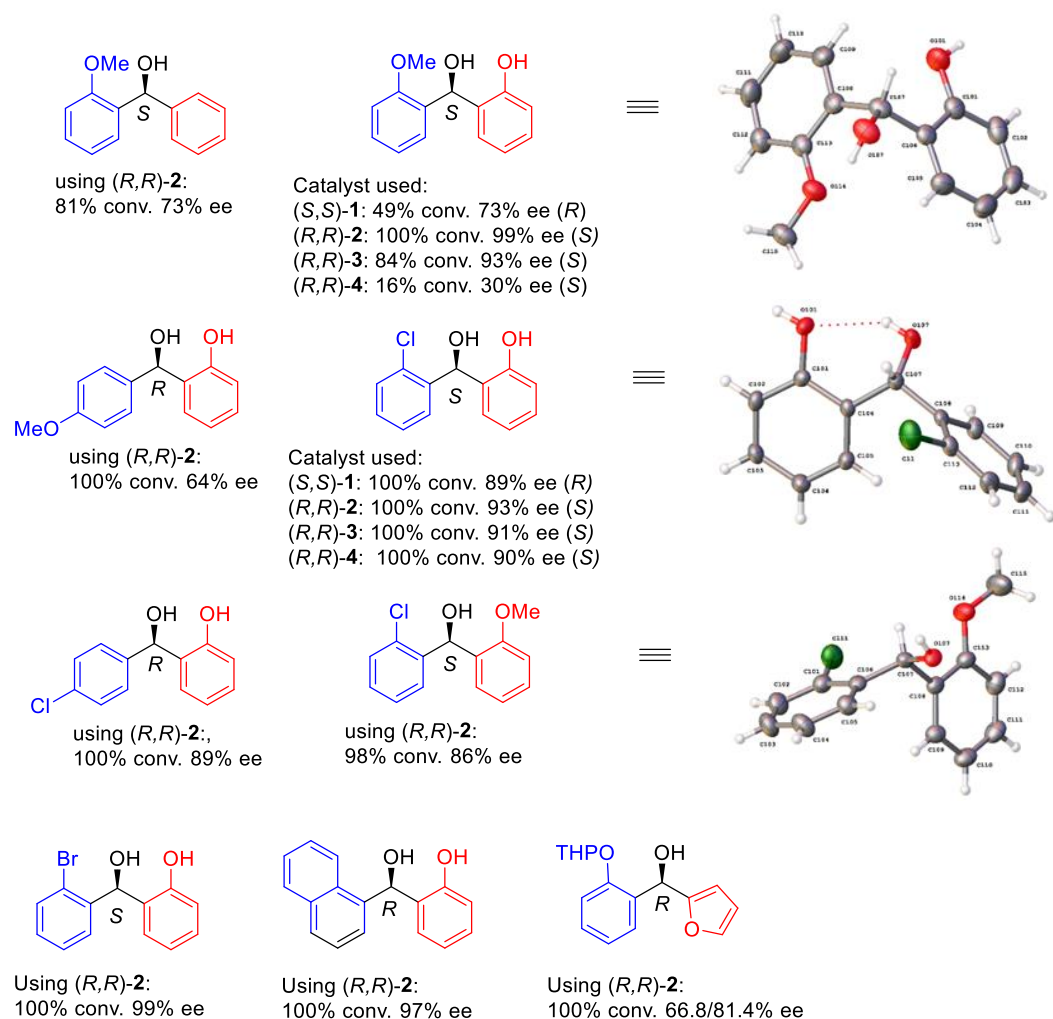
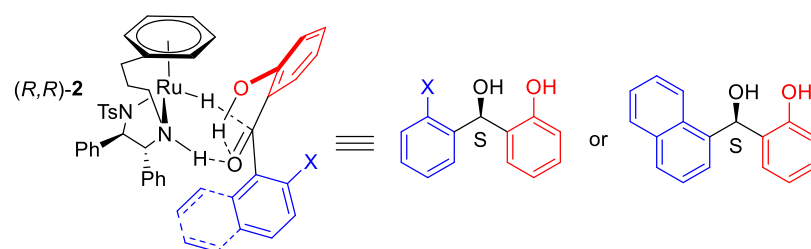
Figure 10. Further examples of ATH of *ortho*-hydroxy benzophenones.

Figure 11. Involvement of H-bond in reduction mechanism.

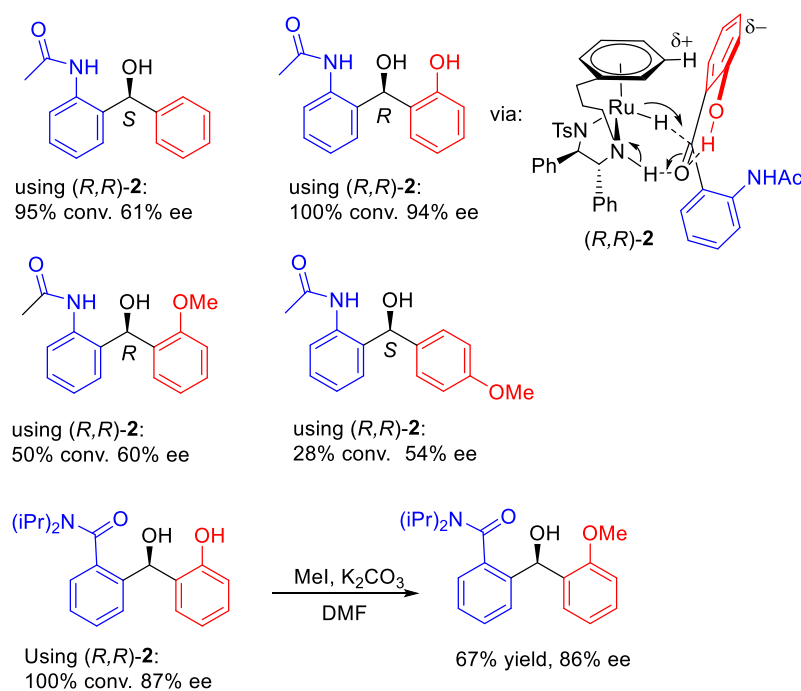


Figure 12. ATH of benzophenones containing amides.

In addition to ketones, imines containing *ortho*-OH group were also studied. However, the hydrolysis of imines is more likely to occur when using FA: TEA (5:2) as the hydrogen source. Thus, the unique condition of ATH of imines with catalyst (*R,R*)-2 is using ammonium formate in DCM at 70 °C in sealed tube under nitrogen atmosphere and only 0.5 mol% catalyst were applied.⁸ Following the earlier precedents (Figure 13), ATH of imines also delivered products of good ees (Figure 14).

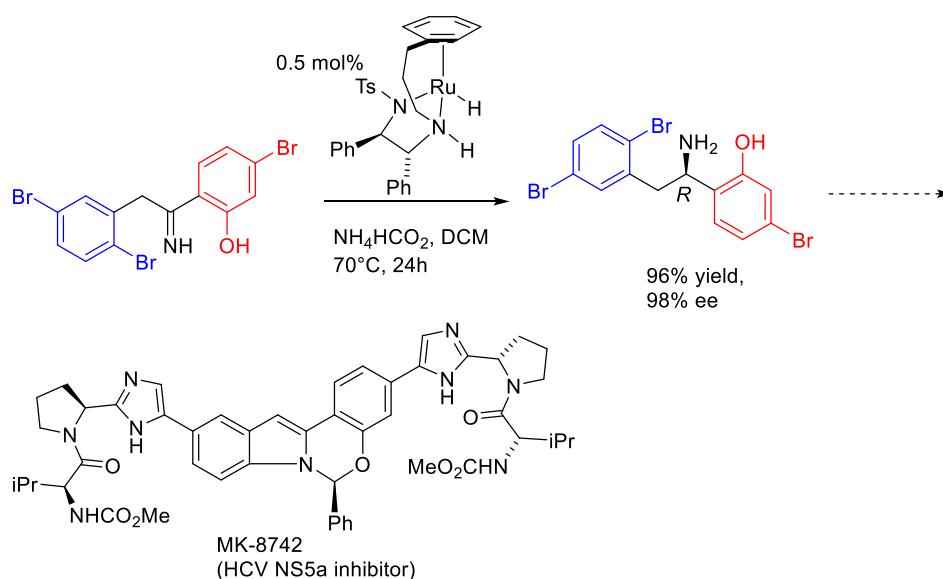


Figure 13. A reported imine ATH using a tethered catalyst.

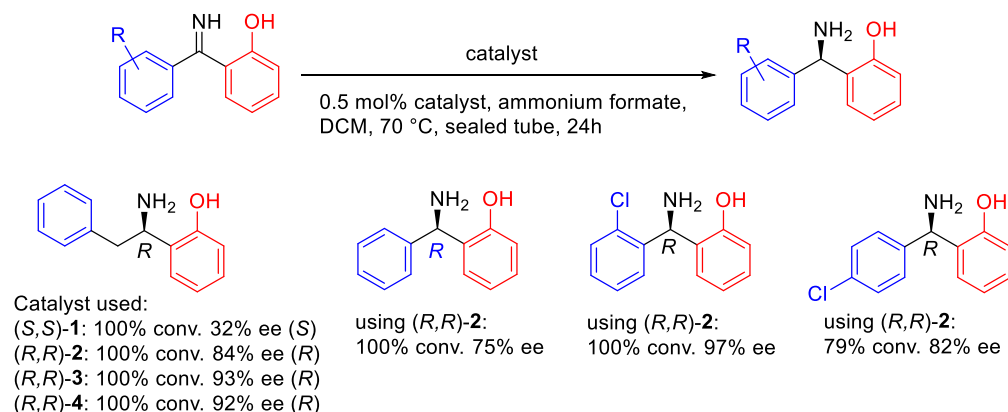


Figure 14. ATH of imines using a tethered catalyst.

The reductions have several potential applications. The *ortho*-hydroxy directing effect can be applied to synthesize highly enantioselective compounds, which can't be made in high ee by direct ATH. In addition, there is also a potential to synthesize pharmaceutically-valuable targets such as a sphingosine 1-phosphate receptor inhibitor precursor with high enantioselectivity by using a Suzuki coupling reaction (Figure 15).

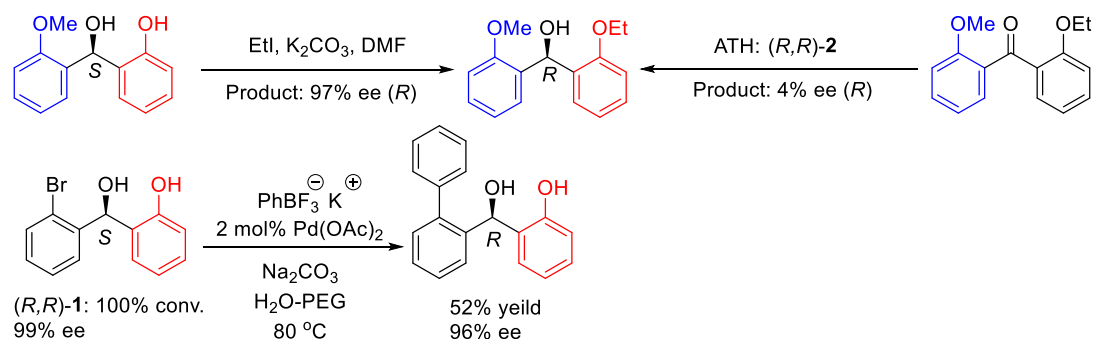


Figure 15. Functionalisations of the ATH products.

ATH of aryl heteroaryl ketones using Noyori-Ikariya catalysts has also been studied (Figure 16).⁹ Four catalysts have been tested for reducing most of the substrates.

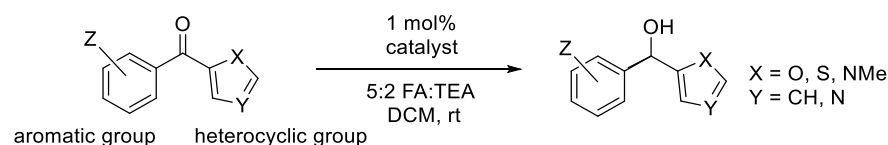


Figure 16. ATH of heterocyclic/aromatic ketones – reported examples.

Ketones where Ar = Ph, *o*-(MeO)C₆H₄ (oOMe), *o*-(Me)C₆H₄ (oMe), *o*-(Br)C₆H₄ (oBr), *o*-(Br)C₆H₄ (oCl) and *n*-naphthyl (Np) versus Het = 2-furyl (Fu), 2-thienyl (Thio), 2-*N*-methylimidazole (Im) and 2-*N*-methylpyrrole (PyMe) were studied. The results indicated that the electron-rich heterocyclic rings are more competitive and adjacent to η^6 -arene ring in transition state (Figure 17).

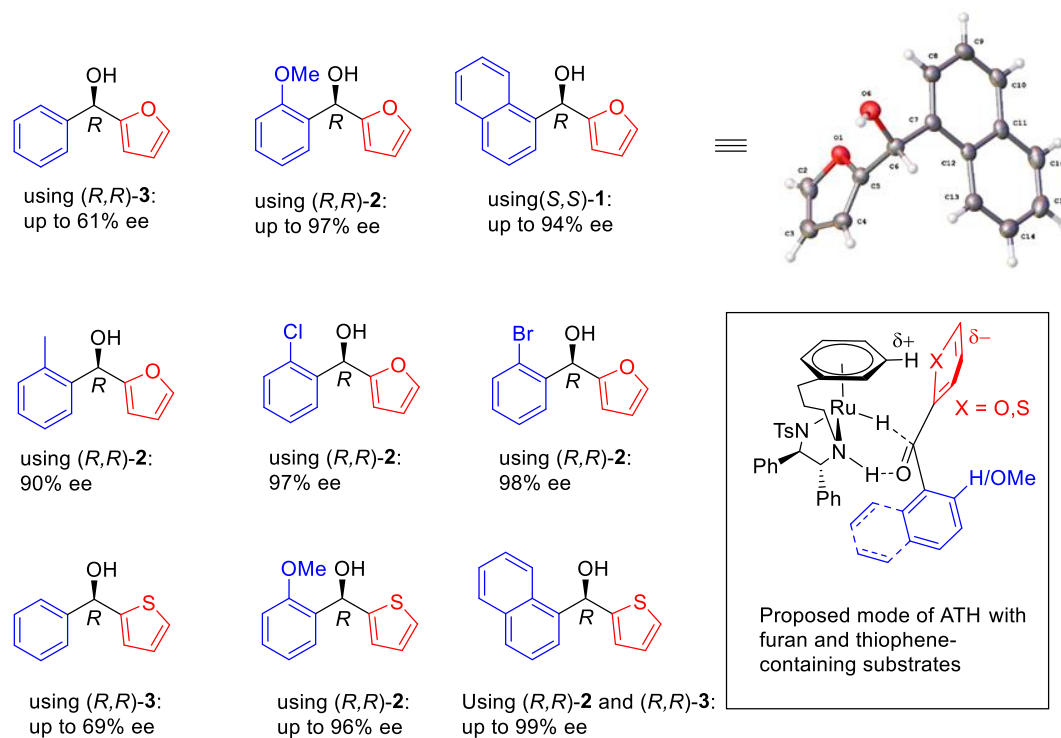


Figure 17. ATH of aromatic/heterocyclic ketones in this product.

For the *N*-methylimidazole-containing ketones, the pattern becomes a little bit complex (Figure 18). The X-ray crystallographic structure of 7 showed it is *R* configuration after ATH with catalyst (*R,R*)-2 and naphthyl ring is out of plane. However, the X-ray crystallographic structure of 8 illustrated the product is *S* configuration, which is also confirmed by methylation and comparison with the HPLC of alcohol 9. Therefore, we proposed transition states for these two substrates (Figure 18). The *N*-methyl imidazole is likely to be protonated under the mildly acidic reaction conditions, so the *ortho*-methoxyphenyl group could be adjacent to η^6 -arene ring as it is more electron rich. However, the bulky naphthyl ring has more steric effect and favours positioning distal to η^6 -arene ring. In addition to compounds 7 and 8, we also studied other substrates with *N*-methylimidazole group and some of them can provide reasonable results although some were resistant to ATH (Figure 19).

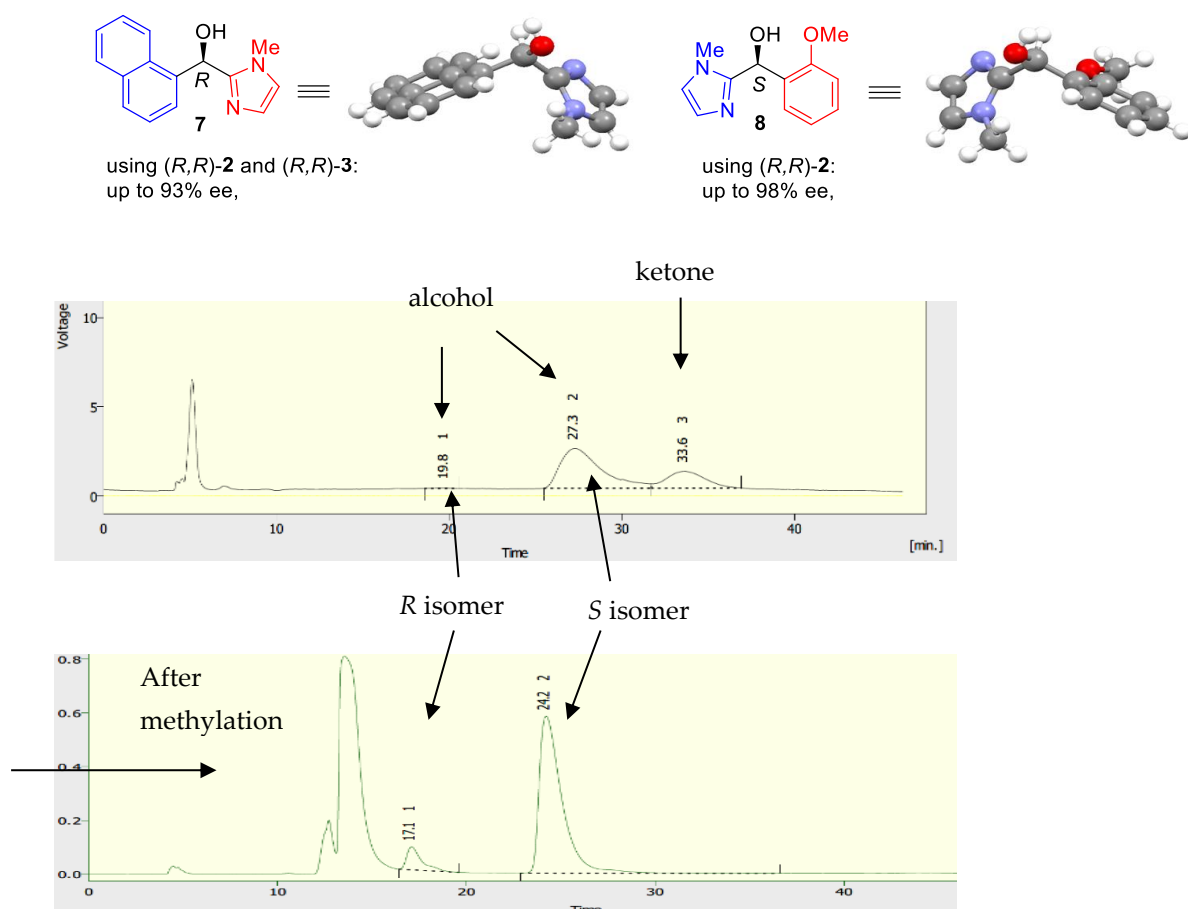


Figure 18. Determination of configuration of ATH products containing imidazole groups.

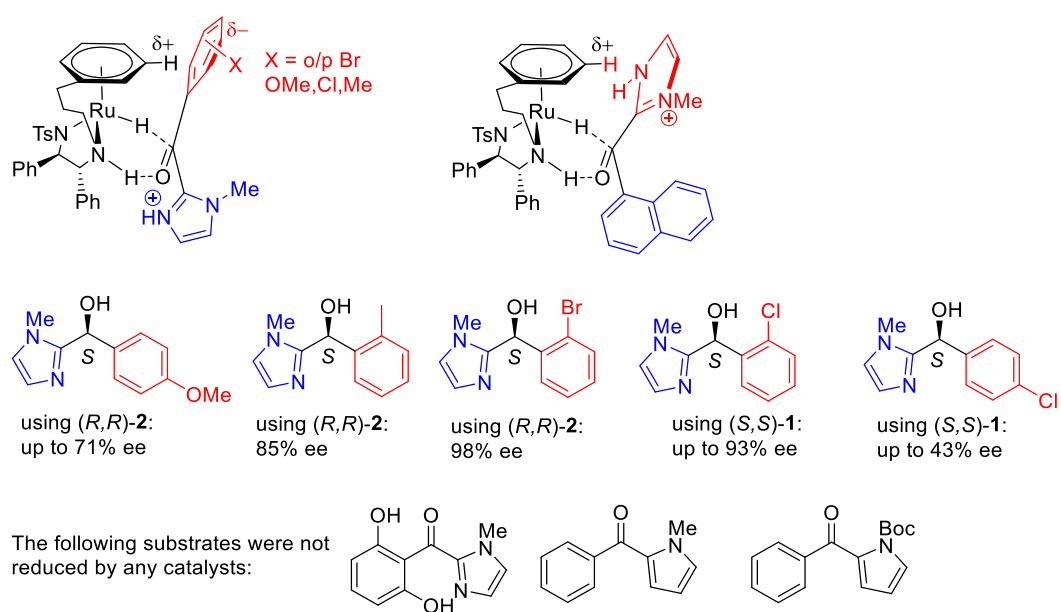


Figure 19. Products of ATH of an extended range of aromatic/heterocyclic ketones, and proposed modes of hydrogen transfer to substrates.

In conclusion,

- (*R,R*)-3C-tethered catalyst 2 was found to be the most active catalyst for ATH of a series of *ortho*-hydroxy benzophenone and aromatic/heterocyclic ketones.
- The enantioselectivity can be influenced by a combination of steric and electronic factors.
- The directing effect of the *o*-OH group in hindered ketones and imines can provide the products with high enantioselectivity.
- The reduction enantioselectivity of a range of ketones flanked by a combination of an aromatic and a heterocyclic ring (furan, thiophene, *N*-methylimidazole) was high (up to 99% ee) in cases where the aromatic ring contained an *ortho*-substituent.

References:

1. a) Hashiguchi, S.; Fujii, A.; Takehara, J.; Ikariya, T.; Noyori, R. *J. Am. Chem. Soc.*, 1995, 117, 7562-7563. b) A. Fujii, S. Hashiguchi, N. Uematsu, T. Ikariya and R. Noyori, *J. Am. Chem. Soc.*, 1996, 118, 2521-2522.
2. a) Dub, P. A.; Ikariya, T. *J. Am. Chem. Soc.* 2013, 135, 2604-2619. b) Dub, P. A.; Gordon, J. C. *Dalton Trans*, 2016, 45, 6756-6781. c) Nedden, H.G.; Zanolli-Gerosa, A.; Wills, M. *Chem Rec*, 2016, 16, 2619-2639. d) Alonoso, D. A.; Brandt, P.; Nordin, S. J. M.; Andersson, P. G. *J. Am. Chem. Soc.*, 1999, 121, 9580-9588. e) Yamakawa, M.; Noyori, R. *Angew. Chem Int. Ed.*, 2001, 40, 2818-2821. f) Dub, P. A.; Henson, N. J.; Martin, R. L.; Gordon, J. C. *J Am Chem Soc*, 2014, 136, 3505-3521. g) Hashiguchi, S.; Noyori, R. *Acc. Chem. Res.*, 1997, 30, 97-102.
3. Noyori, R.; Hashiguchi, S. *Acc. Chem. Res.*, 1997, 30, 97-102.
4. a) Soni, R.; Jolley, K. E.; Clarkson, G. J.; Wills, M. *Org. Lett.* 2013, 15, 5110-5113. b) Soni, R.; Jolley, K. E.; Gosiewska, S.; Clarkson, G. J.; Fang, Z.; Hall, T. H.; Treloar, B. N.; Knighton, R. C.; Wills, M. *Organometallics*, 2018, 37, 48-64. c) Touge, T.; Hakamata, T.; Nara, H.; Kobayashi, T.; Sayo, N.; Saito, T.; Kayaki, Y.; Ikariya, T. *J. Am. Chem. Soc.*, 2011, 133, 14960-14963.
5. a) Noyori, R.; Hashiguchi, S. *Acc. Chem. Res.* 1997, 30, 97-102. b) Touge, T.; Nara, H.; Fujiwhara, M.; Kayaki, Y.; Ikariya, T. *J. Am. Chem. Soc.*, 2016, 138, 10084-10087. c) Vyas, V. K.; Knighton, R. C.; Bhanage, B. M.; Wills, M. *Org. Lett.* 2018, 20, 975-978.
6. a) Wang, B.; Zhou, H.; Lu, G.; Liu, Q.; Jiang, X. *Org. Lett.* 2017, 19, 2094-2097. b) Liu, Q.; Wang, C.; Zhou, H.; Wang, B.; Lv, J.; Cao, L.; Fu, Y. *Org. Lett.* 2018, 20, 971-974. c) Gonzalez-Bobes, G.; Hanson, R.; Strotman, N.; Guo, Z.; Goswami, A. *Adv. Synth. Catal.* 2016, 358, 2077-2082.
7. Zheng, Y.; Clarkson, G. J.; Wills, M. *Org. Lett.* 2020, 22, 3717-3721.
8. Mangion, I. K.; Chen, C. Y.; Li, H.; Maligres, P.; Chen, Y.; Christensen, M.; Cohen, R.; Jeon, I.; Klapars, A.; Krska, S.; Nguyen, H.; Reamer, R. A.; Sherry, B. D.; Zavialov, I. *Org Lett.* 2014, 16, 2310-2313.
9. Zheng, Y.; Martinez-Acosta, J. A.; Khimji, M.; Barbosa, L. C. A.; Clarkson, G. J.; Wills, M. *ChemCatChem*, 2021, 13, 4384-4391.